A Performance Investigation of a Four-Switch Three-Phase Inverter-Fed IM Drives at Low Speeds Using Fuzzy Logic and PI Controllers

L.RAJU
M.TECH IN POWER ELECTRONICS STUDENT
CHAITANYA INSTITUTE OF TECHNOLOGICAL SCIENCES, WARANGAL, TELANGANA

B.BHASKAR
ASSISTENT PROFESSER
CHAITANYA INSTITUTE OF TECHNOLOGICAL SCINCES, DEPT.OF.EEE, WARANGAL, TELANGANA

Abstract: ***This paper presents a speed controller using a fuzzy-logic controller (FLC) for indirect field-oriented control (IFOC) of induction motor (IM) drives fed by a four-switch three-phase (FSTP) inverter. In the proposed approach, the IM drive system is fed by an FSTP inverter instead of the traditional six-switch three-phase (SSTP) inverter for cost-effective low-power applications. The proposed FLC improves dynamic responses, and it is also designed with reduced computation burden. The complete IFOC scheme incorporating the FLC for IM drives fed by the proposed FSTP inverter is built in MATLAB/Simulink, and it is also experimentally implemented in real time using a DSP-DS1103 control board for a prototype 1.1-kW IM. The dynamic performance, robustness, and insensitivity of the proposed FLC with the FSTP inverter-fed IM drive is examined and compared to a traditional proportional-integral (PI) controller under speed tracking, load disturbances, and parameters variation, particularly at low speeds. It is found that the proposed FLC is more robust than the PI controller under load disturbances, and parameters variation. Moreover, the proposed FSTP IM drive is comparable with a traditional SSTP IM drive, considering its good dynamic performance, cost reduction, and low total harmonic distortion (THD).***

KEY WORDS—four-switch three-phase (FSTP) inverter, fuzzy-logic controller (FLC), indirect field-oriented control (IFOC), parameters variation, total harmonic distortion (THD).

I.INTRODUCTION

Three phase induction motors have been considered one of the most commonly used electric machines in industrial applications due to their low cost, simple, and robust construction. Three-phase inverters are considered an essential part in the variable speed ac motor drives. Previously, the traditional six-switch three-phase (SSTP) inverters have been widely used in different industrial applications. These inverters have some drawbacks in low-power range applications, which involve extra cost; the six switches losses, and complicated control schemes. Moreover, they require building interface circuits to produce six pulse width modulation (PWM) pulses [1]–[3]. The development of low-cost motor drive systems is an important topic, particularly for a low-power range. Therefore, the three-phase inverter with reduced component for driving an induction motor (IM) was presented in [1]. Also, reduced switch count has been extended for a rectifier–inverter system with ac-tive input current shaping [2]. Three different configurations of IM drives fed from a four-switch inverter to implement low-cost drive systems for low-power range applications have been presented in [3].

Recently, different research works to design new power con -verters for minimizing losses and costs have been proposed. Four-switch three-phase (FSTP) inverters instead of SSTP in -verters have been used in motor drives [4]–[9], renewable energy applications [10], and active power filters [11], [12]. Control of FSTP brushless dc motor drives has been presented in [4]; us-ing direct torque control (DTC) with no sinusoidal back EMF [5], using single current sensor [6], or using DTC with reduced torque ripples [7]. Compensation of inverter voltage drop in DTC for FSTP PM brushless ac drives has been presented in [8] A DTC strategy for FSTP-inverters with the emulation of the SSTP inverter operation has been presented in [9]. An FSTP inverter has been presented for renewable energy source integration to a generalized unbalanced grid-connected system [10].

Some features of FSTP inverters over the traditional SSTP in-verters have been achieved such as minimized switching losses, decreased cost due to reduction in switches number, reduced number of interface circuits, simpler control schemes to pro-duce logic pulses, low computational burden, and more reliability because of lesser interaction between switches [13]. The PWM method of FSTP inverters has been improved in [13]. However, it requires more voltage sensors. The problem associated with FSTP inverter has been further investigated in [14]. A method to produce PWM pulses to control the FSTP-inverters and compensation of capacitor unbalance has been proposed in [15] A DC–AC FSTP SEPIC-based inverter has been presented in this inverter improves the utilization of the dc bus com-pared to the traditional FSTP inverter. Motor current unbalance of FSTP inverters has been studied with a compensation method utilizing current feedback.

The control of IMs is a challenging issue as a result of their nonlinear model and parameters variation. In classical control systems using proportional-integral (PI) and PI-derivative (PID) controllers, the controller performance is significantly reliant on the IM models. However, most of these models are complicated and parameters dependent. Also, they use some assumptions that cause inaccuracy in the mathematical model. Therefore, the model-based controllers, such as a traditional PI and PID

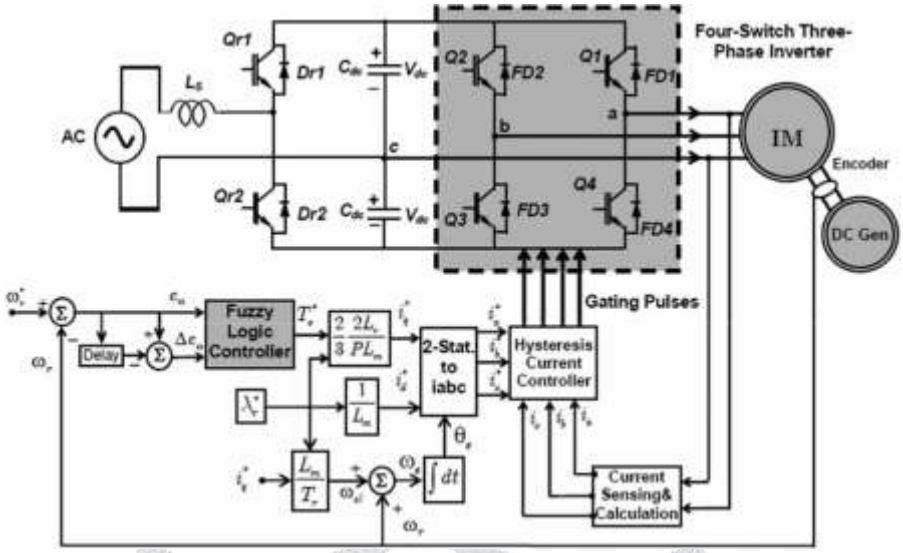

Fig. 1. Block diagram of the proposed FLC-based IFOC scheme of the IM drive fed by FSTP voltage source inverter.

controllers, cannot give satisfactory performance under speed tracking changes, load impact, and parameters variation. Several works to design the speed controller of electrical motor drives to overcome the problem of fixed gains PI controllers are recently proposed such as a sliding-mode control with disturbance compensation , adaptive PID controller, model predictive direct control, online inertia identification algorithm for PI parameters optimization, and a data-based PI controller.

In recent years, extensive research works have been presented to implement artificial intelligent controllers (AICs) owing to their merits compared to classic PI and PID controllers. The major merits of AICs are that they are independent of the plant mathematical model and their performances are robust under system nonlinearities and uncertainties. AICs techniques for SSTP inverters-fed IM drive systems include fuzzy-logic controller (FLC) ,self-tuned neuro-fuzzy controller, emotional intelligent controller, and adaptive fuzzy sliding-mode control. Also, the FLC for IPMSM-based FSTP inverters has been developed in.

The rotor flux is essential for an accurate operation of indirect field-oriented control (IFOC) of IM drives. The field-orientation technique needs precise machine parameters to guarantee accu-rate decoupling of the stator current vector in relation to the rotor flux vector. Using sensors for direct measurement of the rotor flux gives correct value without sensitivity to machine parameters. Nevertheless, this method is problematic, costly, and prone to errors in noisy environments. Therefore, flux es-timation based on the dynamic model of the IM is highly re-quired for high-performance IFOC of IM drives. A problem is that actual machine parameters vary with operating condi-tions. Inaccurate machine parameters may cause torque non-linearity and saturation of the motor. It is possible that the machine control performance degrades due to the parameters mismatch and the system becomes detuned. Consequently, the flux estimation should be as insensitive to varying parameters as possible, which is critical to ensure correct field-orientation control. The flux estimation with its different techniques is a challenge for both speed-sensored and speed-sensorless drives.

In the low-speed region, the effect of changing the motor pa-rameters (stator and rotor resistances as well as the moment of inertia) is considered of utmost importance. For speeds lower than 2/3 maximum motor speed, the performance of FSTP inverters is similar to SSTP inverters because the maximum common-mode voltage from an FSTP is 2/3 of the maximum common-mode voltage from traditional SSTP inverters [3], [15]. Then, the stable operation of FSTP inverters is till 2/3 of the maximum speed. For speeds above 2/3 maximum motor speed, FSTP inverters need extra dc-link voltage to achieve IFOC and develop the same performance of the drive system with SSTP inverters.

Previous works have been reported on the application of the FLC-based IM drive. Also, few works have been presented for the FLC-based IM fed from the FSTP inverter. However, these works were restricted to high-speed region, and low-speed region is not examined. Thus, it is essential to expand FLC-based IM drives during low and high speeds. Also, these works do not provide any results about the effectiveness of the FLC under parameters uncertainty in the low speed region. Therefore, there is a strong need for successful development and real-time implementation of the FLC-based IM fed from FSTP inverter, which will be appropriate for cost-effective low power practical applications. Hence, the most important contribution of this paper compared with other works is to investigate the dynamic performance of FSTP inverter-fed IM drives using the FLC, particularly at low speeds.

This contribution is achieved throughout the following points:

1) investigate the dynamic performance of an FLC-based FSTP inverter-fed IM for high-performance industrial ap-plications under speed tracking, load disturbance, and pa-rameters variation, particularly at low speeds;

2) implement the complete IFOC technique of an IM drive fed by the proposed FSTP inverter in MATLAB/Simulink, and also, in real time by a DSP-DS1103 control board for a prototype 1.1-kW IM;

3) verify the robustness of the proposed FLC in compari-son to the traditional PI controller using simulation and experimental results at different operating conditions;

4) examine the insensitivity of the two controllers to param-eters variation, particularly motor inertia and stator and rotor resistances;

5) Compare the performance of the proposed FSTP inverter and the SSTP inverter using total harmonic distortion (THD) of the stator current.

II. MOTOR DYNAMICS AND CONTROL SCHEME

A. Mathematical model of IM and Control Scheme

The representation of the IM in a $d-q$ axis was used, and the control structure relies on the IFOC. Detailed explanation of the IFOC model was presented in for non-repetition. The control structure of the proposed FLC-based IFOC of the IM fed by the FSTP voltage-source inverter (VSI) is illustrated in Fig. 1. The speed error between the reference and actual motor speeds and the derivative of speed error are the inputs to the FLC and its output is the reference torque T_e^*. The reference currents in d–q axis are transformed into the reference motor currents in a–b–c axis by inverse Park's transformation. The differences between reference motor currents and their actual values are the inputs to hysteresis bands of the current-controlled VSI to generate PWM binary signals, which are utilized to activate the switches of the FSTP inverter. The motor voltages are then produced using the switching states of the FSTP inverter and the dc-link voltage.

B. FSTP Inverter

The power circuit of an FSTP-VSI-fed IM is illustrated in Fig. 1. This circuit is composed from two sides. The first side is a half-wave voltage doubler fed from a single-phase ac power supply. The frequency of the input ac voltage is fixed; this volt-age is rectified using rectifier switches Qr1 and Qr2. The recti-fier circuit is utilized to charge the capacitor bank in the dc link. The second side is the FSTP-VSI. The FSTP inverter utilizes four switches: Q1, Q2, Q3, and Q4, respectively, as illustrated in Fig. 1. Phase "a" and phase "b" of the IM are connected through two limbs of the inverter, while phase "c" is connected to the midpoint of the capacitors bank. The FSTP inverter uses four isolated gate bipolar transistors (IGBTs) and four freewheeling diodes to get the two line-to-line voltages V_{ac} and V_{cb}. However, the third line to line voltage (V_{ba}) is obtained using Kirchhoff's voltage law from a split capacitor bank. The maximum dc-link voltage across each capacitor is equal to V_{dc}. The generated three-phase output voltages using an FSTP inverter are balanced with adjustable voltage and frequency. In the current analysis, the FSTP inverter switches are considered as ideal switches. The three-phase output voltages of the FSTP inverter are obtained using the dc-link voltages V_{dc} and the binary signals of the two limbs of the FSTP inverter. The generated phase voltages-fed IM can be expressed as a function of the switching states of the

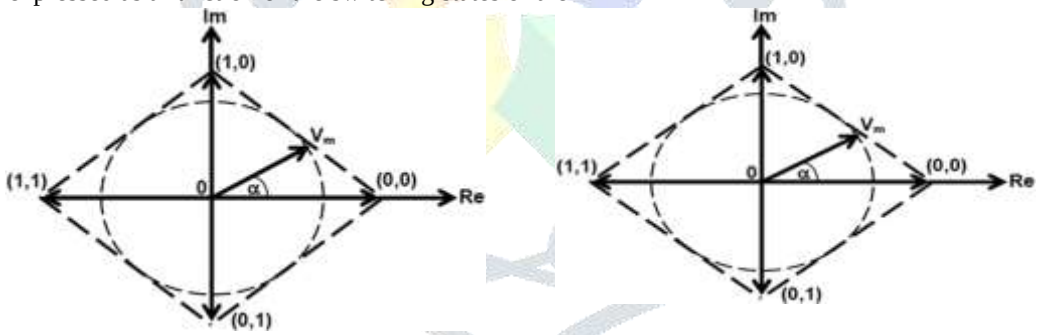

Fig. 2. Switching vectors for an FSTP voltage source inverter.

I TABLE

FSTP INVERTER MODES OF OPERATION

Switching Function		Switch ON		Output Voltage Vector		
S_a	S_b			V_a	V_b	V_c
0	0	Q_4	Q_3	$-V_{dc}/3$	$-V_{dc}/3$	$2V_{dc}/3$
0	1	Q_4	Q_2	$-V_{dc}$	V_{dc}	0
1	0	Q_1	Q_3	V_{dc}	$-V_{dc}$	0
1	1	Q_1	Q_2	$V_{dc}/3$	$V_{dc}/3$	$-2V_{dc}/3$

inverter and V_{dc} as follows [30]:

$$V_a = \frac{c}{3}(4S_a - 2S_b - 1)V_d$$
$$V_b = \frac{c}{3}(-2S_a + 4S_b - 1)V_d \quad (1)$$
$$V_c = \frac{c}{3}(-2S_a - 2S_b + 2)V_d$$

where V_{dc} is the peak voltage across the storage capacitors; S_a and S_b are the actual states of the two phases "*a*" and "*b*" represented by two binary logic variables, which determine the conduction state of the inverter. When S_a is 1, switch (Q1) is conducted and switch (Q4), is not, and when S_a is 0, switch (Q4) is conducted and switch (Q1) is not. S_b has the same principle of operation, and V_a , V_b , and V_c are motor phase voltages.

For the balanced generated voltages, the four actual combi-nations of the inverter status are lead to four voltage vectors as shown in Fig. 2. Table I illustrates the possible modes of operation and the generated output voltage vector of the FSTP inverter as in.

Fig. 3(a) illustrates the simulation study of phase-*a* current in steady state and its THD at speed 50 r/min under rated load conditions using a PI controller with an FSTP inverter-fed IM drive. To provide a fair comparison, the simulation study of steady-state phase-*a* current and its THD using an FLC with the FSTP-inverter-fed IM drive at similar test conditions are illustrated in Fig. 3(b). It is observed that the motor phase-*a* current in steady state and its THD of the proposed FLC with the FSTP-inverter-fed IM drive has less THD compared with the traditional PI controller. Also, the simulation tests of the phase-*a* current in steady state and its THD at speed 50 r/min under rated load conditions using the FLC with an SSTP inverter-fed IM drive is illustrated in Fig. 3(c). It is noted that the FLC usin

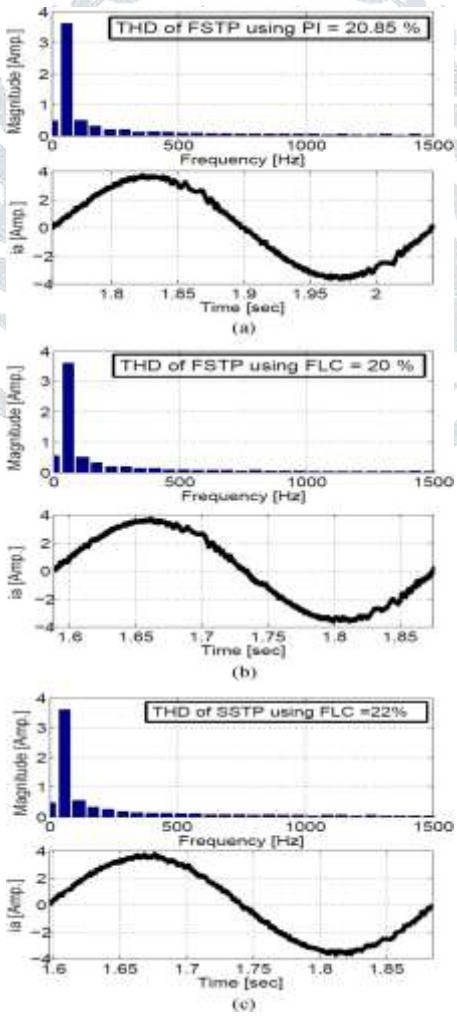

Fig. 3. Simulation results of steady-state phase current i_a and its harmonic spectrum at speed 50 r/min under rated load conditions using: (a) PI controller-based FSTP inverter-fed IM drive; (b) FLC-based FSTP inverter-fed IM drive; and (c) FLC-based SSTP inverter-fed IM drive.

FSTP inverter-fed IM drive gives less THD compared to the FLC with the traditional SSTP inverter-based method.

III. SPEED CONTROL METHODS

A. FLC Algorithm

The FLC is used with an IM to overcome the problem of developing accurate mathematical description due to load disturbances and parameters changing. The inputs to the FLC block are the deviation between the reference and actual mo-tor speeds (speed error) and speed error derivative. These two inputs are utilized to produce the command torque of an IM (output of the FLC). As illustrated in Fig. 1, the reference torque and reference flux are used to calculate the two refer-ence current components in quadrature and direct axis (i^*_q , i^*_d), respectively. These two currents in combination with the unit vector value are utilized to calculate the three phase reference currents (i^*_a , i^*_b , i^*_c) based on inverse Park's transformation in order to keep the required speed. The main function of the FLC is to keep the motor speed aligned with the desired speed, as a result, the motor currents are kept close to their reference cur-rents. The exact calculations of reference torque depend on the accurate mathematical model of an IM as well as its parame-ters that are really not constant during the motor operation. The effect of motor parameters variation is only noticeable at low speed of operation, which is considered as a big challenge for accurate calculation of the reference torque, as well as the ex-act operation of an IM under the vector control technique. The intelligent controllers, especially an FLC are used with an IM drive to overcome the parameters variation at low-speed oper-ation. The FLC has many features such as, no need for exact mathematical model of an IM, and its action depending on lin-guistic rules with "IF," "AND," and "THEN" operators. This concept is based on the human logic. The main drawback of the FLC is that it needs high calculation burden for simulation and experimental implementations. Therefore, this paper over-comes this problem by designing an FLC with low computation burden. Many membership functions (MFs) shapes can be cho-sen based on the designer preference and experience. These MFs are characterized by a Gaussian membership. The human perception and experience can be implemented through the MF and fuzzy rules [18].

B. Design of Simplified FLC for IM Drive

The dynamic model of IM expressed as follow:

$$T_e = J\frac{d\omega_r}{dt} + B\omega_r + T_L \qquad (2)$$

$$T_e - T_L = J\frac{d\omega_r}{dt} + B\omega_r \qquad (3)$$

$$\frac{d\theta_r}{dt} = \omega_r \qquad (4)$$

where J is the rotor inertia, T_e is the electrical torque, T_L is the load torque, B is the frication damping coefficient, and ω_r is the motor speed. Employing the small-signal model of an IM, it can be seen that a small change of electrical torque T_e results in a small change of the rotor speed ω_r . The electrical motor torque equation rewritten as

$$T_e = J\frac{d\ \omega_r}{dt} + B\ \omega_r + T_L \qquad (5)$$

The model of small signal in discrete time for the simplified IM model with applying constant load expressed as

$$T_e(n) = J\ e(n) + B\ \omega_r(n) + T_L\ . \qquad (6)$$

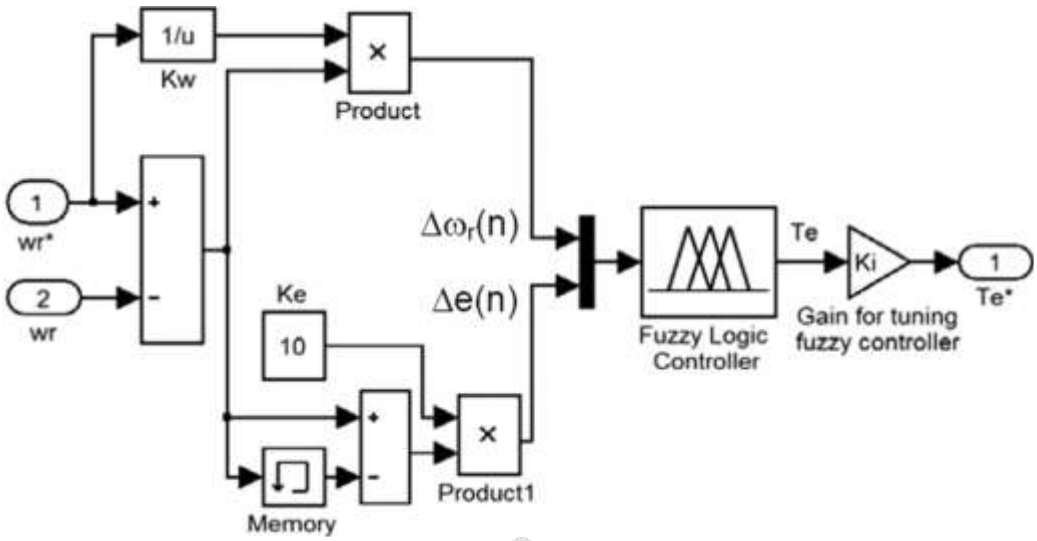

Fig. 4. Block diagram of the FLC using memory block instead of derivative block.

This equation describes the developed electrical torque as a function of motor speed error and change of error as follows:

$$T_e(n) = \sum_{n=1}^{N} T_e(n) = f(\Delta e(n), \omega_r(n)) \quad (7)$$

where N is the total number of rules.

$\omega_r(n) = \omega^*(n) - \omega_r(n)$ is the speed error;

$e(n) = \omega_r(n) - \omega_r(n-1)$ is the change of speed error;

$\omega_r(n-1)$ is the previous sample of speed error;

$\omega_r(n)$ is the current value of speed error, $\omega_r(n)$ is the cur-rent value of motor speed, and $\omega_r^*(n)$ is the present sample of reference motor speed. A MATLAB/Simulink implementation of the FLC is illustrated in Fig. 4. The FLC algorithm of the speed controller employed in the IM drive is based on estimation of two inputs, speed error, and its change as illustrated in Fig.

4. These two linguistic variables are considered as inputs to the system of accordingly interconnected fuzzy-logic (FL) block, and the output is the electrical torque command. The derivative block can be replaced by time-delay block, which is another way to get the required input. This time-delay block would allow shortening the calculation burden, at the same time also secure the controller from uncertainties in the form of spikes in the out-put, which are the drawback of the time-derivative block, if the processed signal change abruptly. The time-delay block would provide a faster and acceptable robust response and as well as precisely accurate tracking of reference speed. It also allows raising the speed sensor sampling rate significantly.

1) Fuzzification Process: To design the proposed FLC, the first step is to choose the scaling parameters $K\,w$, $K\,e$, and $K\,i$, which are determined for the fuzzification process and receiving the suitable values of the reference torque. The parameters $K\,w$ and $K\,e$ are determined so that the normalized value of speed error and its change, $\omega_r(n)$ and $e(n)$, respectively, stays in acceptable limits ±1. The parameter for the output signal $K\,i$ is determined so that the rated torque is the output of the FLC at all rated operations. For implementation, the following values are determined $K\,w = 1/\omega_r^*$ (command speed), $K\,e = 10$, and $K\,i = 10$ in order to obtain the optimal drive simulations and real-time performance. These parameters can

be constants or variables and has a significant role for the FLC design in order to obtain a good response during all operating conditions,

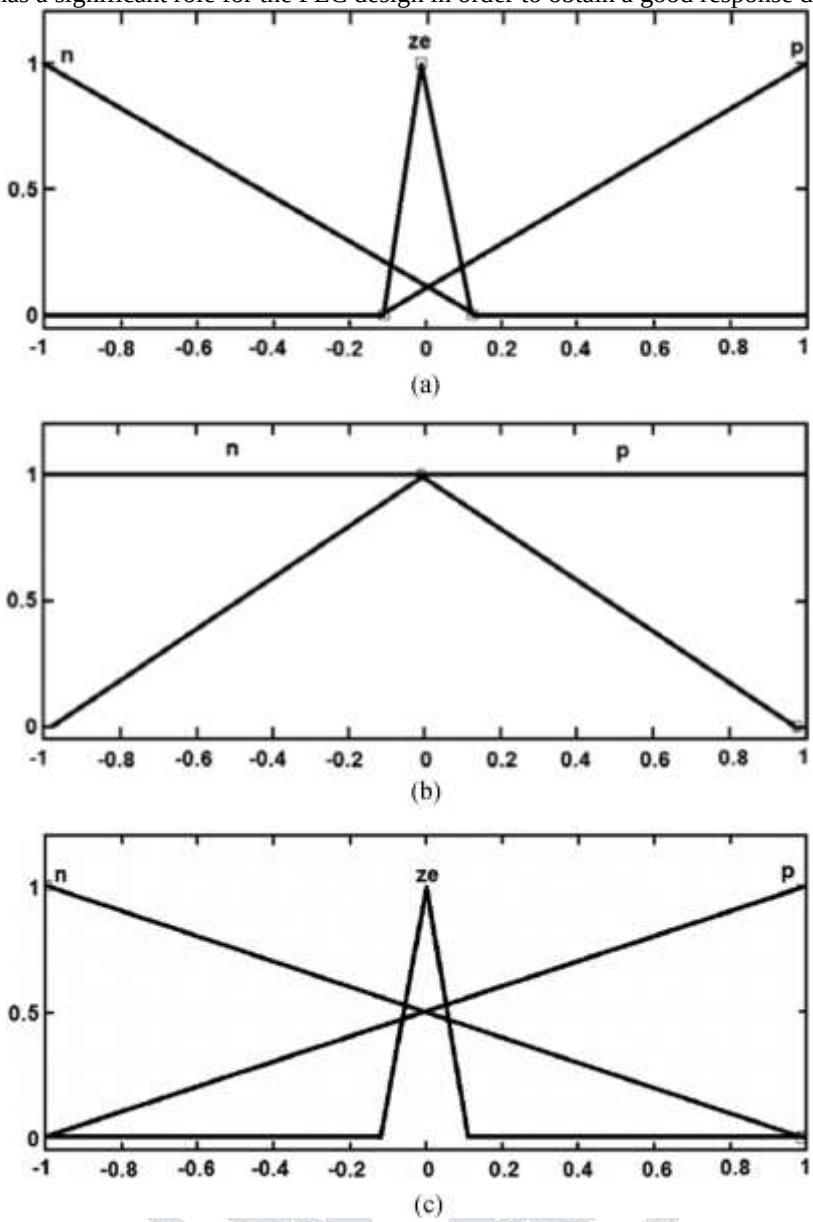

Fig. 5. Membership functions for: (a) speed error ω_r (n); (b) change of speed error $e(n)$; and (c) torque reference T_e (n) implemented in MATLAB Simulink.

In this paper, these parameters are considered constants and are selected by experimental trial and error to achieve the bestpossible drive implementation. The MF's of ω_r (n), e(n), and T_e (n) are chosen after selecting scaling parameters. MF's are important elements of the FLC. Fig. 5 shows the MFs used for the input and output fuzzy sets of the FLC for producing the reference torque. The triangular MF's are utilized for all the fuzzy sets of the input and output vectors because of their ease of mathematical representation. As a result, they simplify the implementation of the FL inference engine and to reduce the computational burden for real-time operation.

2) Rules Base Process: The margin of universe of discourse

of the input vectors ω_r (n) and e(n) and output T_e (n) are chosen from –1 to 1. The exact fuzzy rule base of the simplified FLC of the input variables to the output is done by fuzzy IF-AND-THEN logic operators rules of six linguistic expressions as described in Table II.

3) Inference and Defuzzification: Fuzzy inference is the complete process of formulating the mapping of the function from a given input to an output using FL operators. The Mam-dani and Sugeno are the two basic types of fuzzy inference

TABLE II

RULES BASE PROCESS

1-	IF	$\omega_r(n)$ is N (Negative) AND	$e(n)$ is N (Negative)
	THEN	$T_e(n)$ is ZE (Zero)	
2-	IF	$\omega_r(n)$ is ZE (Zero) AND	$e(n)$ is N (Negative)
	THEN	$T_e(n)$ is P (Positive)	
3-	IF	$\omega_r(n)$ is P (Positive) AND	$e(n)$ is N (Negative)
	THEN	$T_e(n)$ is P (Positive)	
4-	IF	$\omega_r(n)$ is N (Negative) AND	$e(n)$ is P (Positive)
	THEN	$T_e(n)$ is ZE (Zero)	
5-	IF	$\omega_r(n)$ is ZE (Zero) AND	$e(n)$ is P (Positive)
	THEN	$T_e(n)$ is ZE (Zero)	
6-	IF	$\omega_r(n)$ is P (Positive) AND	$e(n)$ is P (Positive)
	THEN	$T_e(n)$ is P (Positive)	

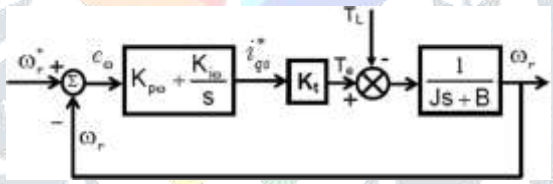

Fig. 6. Block diagram for the speed controller of the IM drive.

methods. The main difference between these types is the way of defining the output. This paper uses the commonly used method for fuzzy inference and defuzzification process, which is Mam-dani max–min (or sum product) composition with the center of gravity method [40]. This method is applied for defuzzification to get $T_e(n)$.

C. Design of the PI Controller

Selection of the PI controller parameters will influence the speed response, its settling time, overshoot value, and load torque rejection, so they should be adjusted to have optimal re-sponse for a fair comparison with the proposed FLC. However, the design of these gains cannot achieve all these characteristics simultaneously as reported in.

To design the PI controller, the schematic diagram of the speed controller of the IM drive is illustrated in Fig. 6. The open-loop transfer function of (8) has one zero at $-K_{i\omega}/K_{p\omega}$, and two poles at zero and $-B/J$. The PI controller parameters are designed to have optimal response using the root-locus method for pole-zero locations as clarified in Fig. 7. The root-locus plot has been used to select the gains of $K_{i\omega}$ and $K_{p\omega}$ to give the required performance. It is found that the PI gains are $K_{i\omega} = 15$ and $K_{p\omega} = 8$ to give the best dynamic response

$$G_{OL}|_{TL=0} = \frac{K_{p\omega} K_t \left(s + \frac{K_{i\omega}}{K_{p\omega}}\right)}{(Js + B)s} \quad . \qquad (8)$$

IV. SIMULATION RESULTS

To validate the effectiveness of the FL speed controller for the FSTP based-IM drive, a simulation model is built by MAT-LAB/Simulink. The dynamic performance of the proposed IM drive system has been examined using simulation results under various operating conditions. A fair performance comparison

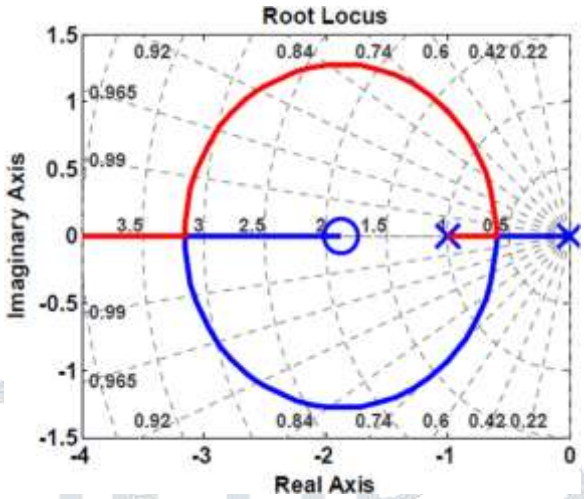

Fig. 7. Root locus plot of the open-loop transfer function with the PI controller gains $K_{p\,\omega}$ = 8 and $K_{i\,\omega}$ = 15.

between the classical PI controller and the proposed FLC is also provided at identical conditions. The parameters of the IM are given in Table IV.

A. Speed Tracking Performance

Fig. 8(a) and (b) demonstrates simulated speed and current signals of the FSTP inverter-fed IM drive using the traditional PI controller and the proposed FLC scheme, respectively, to see the starting performance. The IM drive starts under light-load torque and a speed command changed from 0 to 100 r/min. As shown in Fig. 8(b), the IM drive using the FLC tracks the desired speed smoothly without any overshoot, undershoot, and steady-state error, while the traditional PI controller has an overshoot and large rising time to arrive the desired speed as shown in Fig. 8(a). However, according to Fig. 8(a) and (b), the stator currents show an overshoot but it lasts for only 0.033 s and its value in the PI controller is higher than the FLC.

Other simulated speed and stator current responses at a sud-den speed change are depicted in Figs. 9 and 10 for both the traditional PI controller and FLC. Also, in these cases, the FLC-based IM drive ensures the efficacy over the traditional PI con-troller as the actual speed does not has any overshoot, under-shoot, and steady-state error as shown in Figs. 9(b) and 10(b) when compared with the same [see Figs. 9(a) and 10(a)] us-ing the traditional PI controller. Thus, the FLC-based IM drive fed from the FSTP inverter proves a good performance under speed reference tracking.

B. Load Torque Disturbance

The robustness of an FSTP inverter-fed IM drive for both the traditional PI controller and FLC is also examined for sudden load change at a speed reference 20 r/min as shown in Fig. 11. At $t = 2$ s, a rated torque of 7 N·m is applied. It is found that the FLC-based IM drive system confirms the effectiveness over the traditional PI controller as the actual speed has a low speed dip and recovers quickly with minimum time during sudden load torque, whereas the stator current rapidly arrives to the

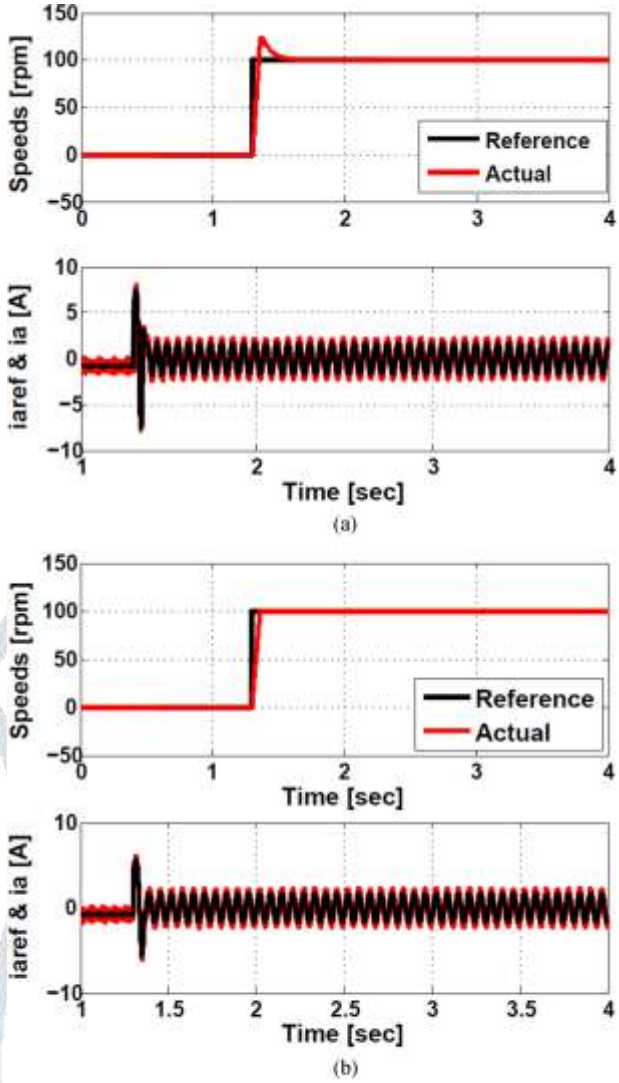

Fig. 8. Simulated speed and stator currents responses of an FSTP inverter-fed IM drive for a starting operation at low speed with a step change of a speed reference from 0 to 100 r/min using (a) traditional PI controller and (b) proposed FLC.

new equivalent value of the rated torque. Therefore, good speed tracking performance and good load torque rejection is attained using the FLC-based IM drive, while the PI-controller-based IM drive is incapable of achieving the desired performance under the sudden change in the reference speed and torque disturbance.

C. Effect of Parameters Variation

The two speed controllers are examined at low speeds under parameters variation. Fig. 12(a) and (b) shows the simulated responses of speed, stator currents, and a quadrature current of an FSTP inverter-fed IM drive for a sudden increase in stator and rotor resistances at a speed reference 20 r/min using the traditional PI controller and FLC. The mismatch of 100% in the stator and rotor resistance values is tested to prove the robustness of the FLC. The first graph of Fig. 12(b) shows the simulated reference and actual speeds. It is observed that the actual speed tracks the reference speed in spite of stator and rotor resistance

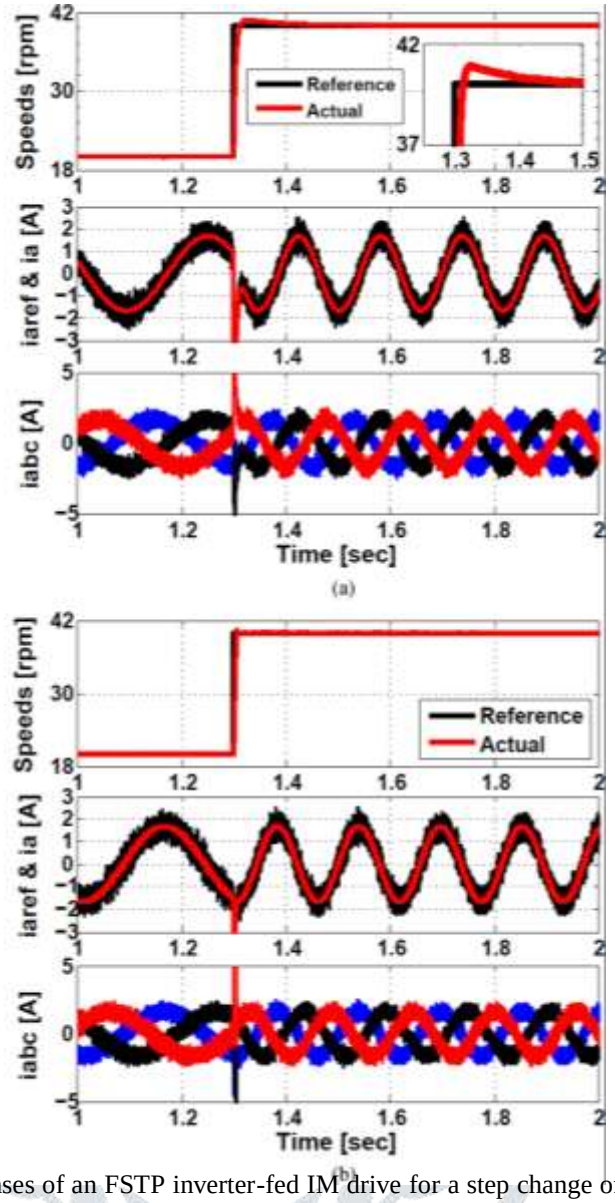

Fig. 9. Simulated speed and stator currents responses of an FSTP inverter-fed IM drive for a step change of a speed reference from 20 to 40 r/min using (a) traditional PI controller and (b) proposed FLC.

mismatches using the proposed FLC. The next graph shows the stator current. It is clear that the frequency of stator current is changed due to the increase of the slip speed at time t = 1.5 s due to the effect of changing the rotor and stator resistances. The third graph shows the q-component current i^*_q . It is found that the current i^*_q shows insignificant changes at time t = 1.5 s for the mismatches in the rotor and stator resistances. The fourth graph demonstrates the mismatch of 100% in the stator and rotor resistance values that are introduced in the simulation model of the IM at time t = 1.5 s. It is evident in the first graph that the proposed FLC is robust under parameters mismatch and the speed tracking is not affected. However, the first graph of Fig. 12(a) exhibits a small variation in the speed under the variation of stator and rotor resistances

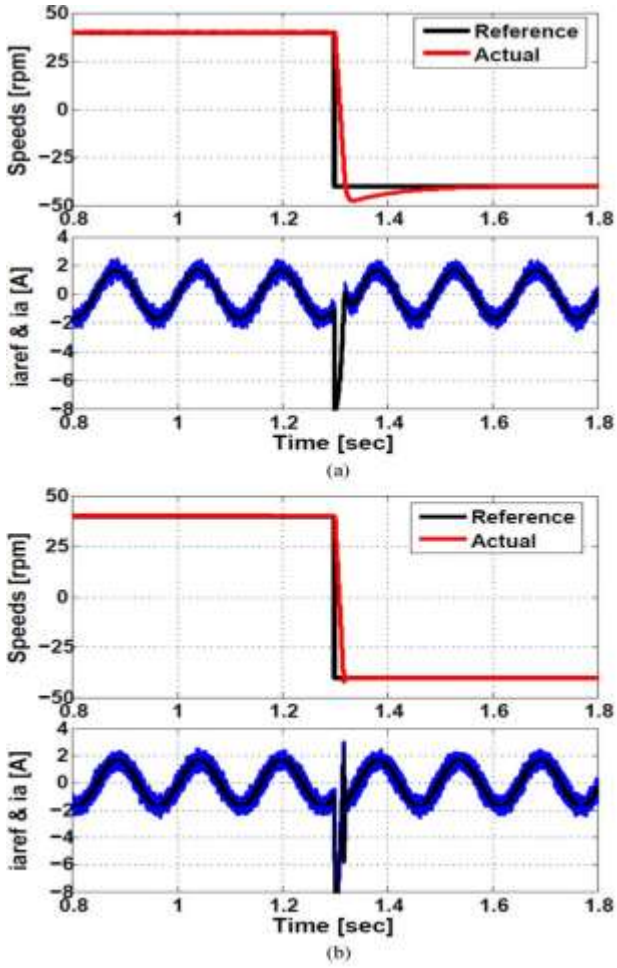

Fig. 10. Simulated speed and stator currents responses of an FSTP inverter-fed IM drive for a speed reversal from 40 to -40 r/min using (a) tradi-tional PI controller and (b) proposed FLC.

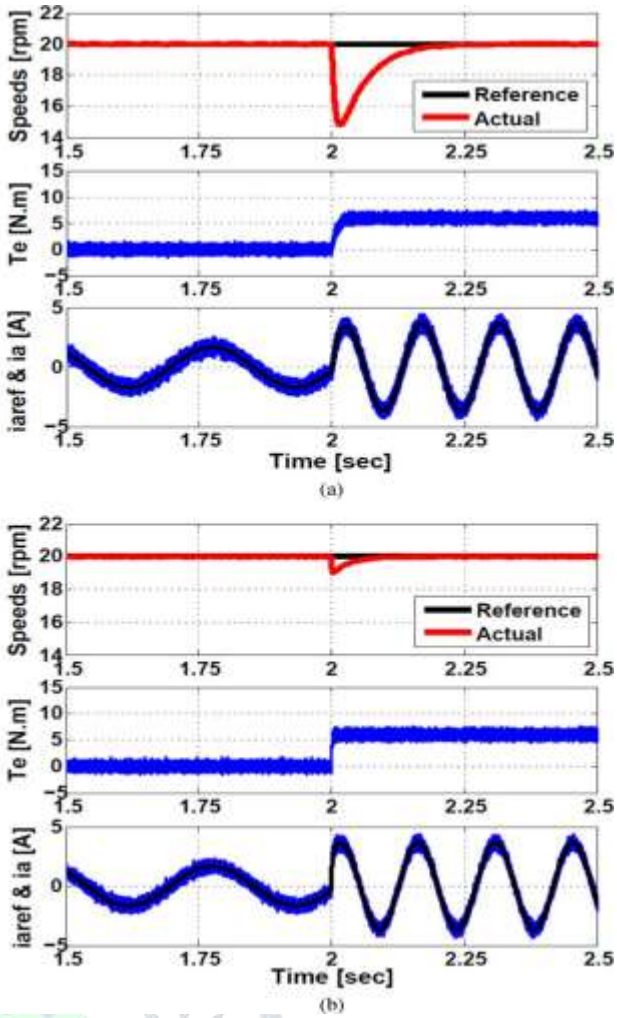

Fig. 11. Simulated speed and stator currents responses of an FSTP inverter-

fed IM drive for a sudden increase in load of 7 N·m at a speed reference 20 r/min
using (a) traditional PI controller and (b) proposed FLC.

Other simulated responses under inertia variation are also pre-sented to examine the robustness of the two speed controllers. The IM drive is tested with inertia ($J = 1.5J_o$). Fig. 13(a) illus-trates simulated speed and trajectory tracking responses of an FSTP inverter-fed IM drive under motor inertia variations for a speed reference of 20 r/min using the traditional PI controller. The same figure at identical conditions is depicted using the proposed FLC for performance comparison purposes as seen in Fig. 13(b). Fig. 13 justifies the robustness of the proposed FLC in comparison to the traditional PI controller. As clear, the traditional PI controller has a substantial variation in the speed response at $J = 1.5J_o$. However, the proposed FLC remains in-sensitive under the identical inertia variation. The phase plane trajectory of the second graph in Fig. 13(a) and (b), validates this superiority of the proposed controller.

EXPERIMENTAL SETUP AND RESULTS

A. Drive System Setup

The behaviors of the proposed FLC-based IM control have been evaluated using Simulink benchmark, and then, verified by experimental implementation in real time using digital signal processing (DSP-DS1103) control card for a laboratory 1.1-kW IM as illustrated in Fig. 14. The parameters of the used IM are listed in Table IV in the appendix. The IM is supplied by FSTP-VSI using four IGBT's and a gate driver board. The control is done using DSP-DS1103 control board, which is interfaced with a personal computer (PC) through the control panel. This panel contains a lot of peripherals such as digital-to-analog (D/A), analog-to-digital (A/D) converters, and position encoder

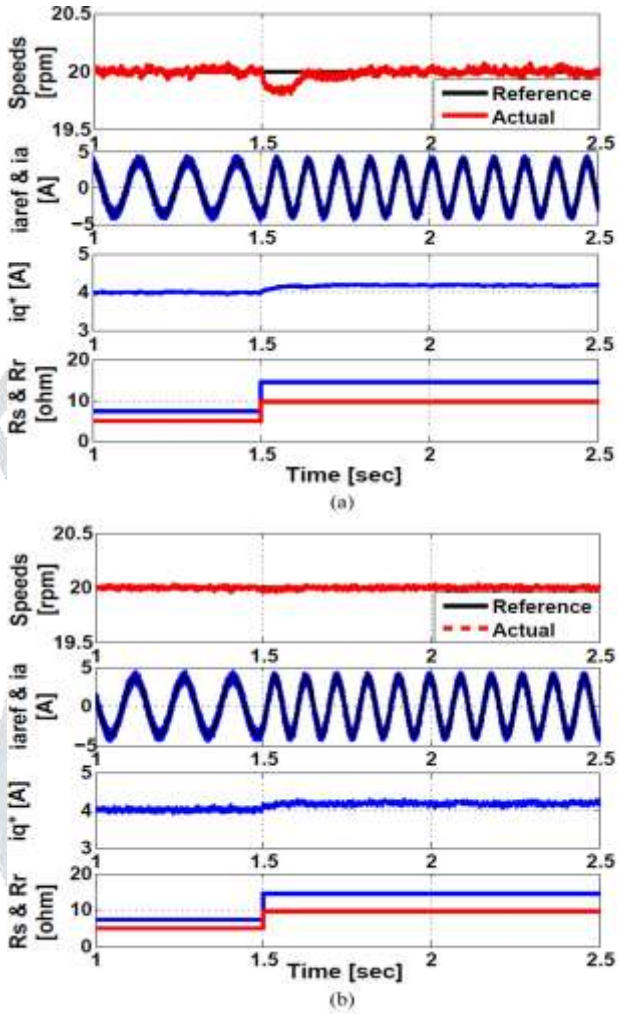

Fig. 12. Simulated speed, stator currents, and quadrature current responses of an FSTP inverter-fed IM drive for a sudden increase in stator and rotor resistances at a speed reference 20 r/min using (a) traditional PI controller and (b) proposed FLC.

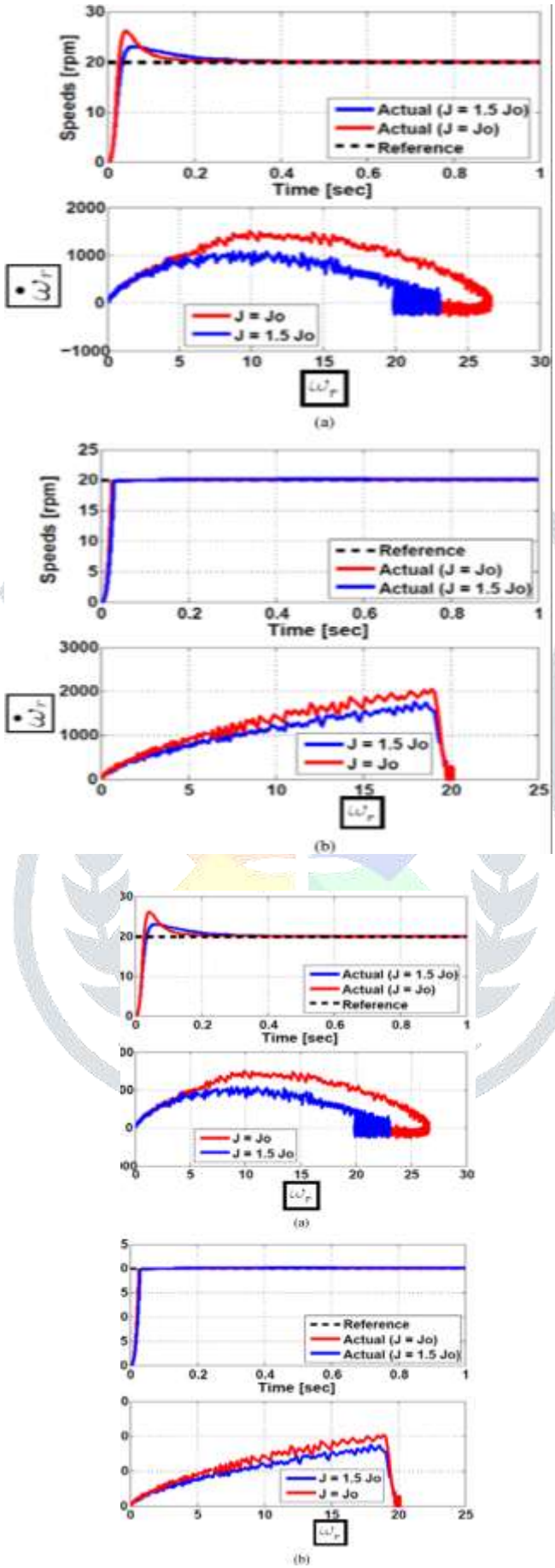

Fig. 13. Simulated speed and trajectory tracking responses of an FSTP inverter-fed IM drive under motor inertia variations for a speed reference of 20 r/min using (a) traditional PI controller and (b) proposed FLC

interfaces. It also provides the required digital input/output (I/O) ports and timer function such as input, output captures, and generation of inverter pulses. All computations are done and programmed on Simulink benchmark through a PC. The real-time Simulink model is built and downloaded to MATLAB environment through the DSP-DS1103 control boad

The inverse Park's transformations are used to obtain the three-phase reference motor currents from the reference direct and quadrature axis currents. The motor currents are measured using the current transducers as inputs to the DSP control board. The hysteresis current controller utilizes the difference between the actual motor currents and the corresponding reference motor currents to produce the four PWM pulses to operate the FSTP inverter. The output voltages from the FSTP inverter are utilized

to supply the IM with suitable voltages and frequency corre-sponding to the operating condition. An incremental encoder with 1024-pulses resolution is used to sense the rotor position and speed. This encoder is interfaced with DSP-DS1103 through the control panel terminals. The IM is connected to a dc gener-ator for mechanical loading. Fig. 15 shows a laboratory picture of an IM drive system.

B. Experimental Results

Samples of the experimental verifications are illustrated to verify the simulation results as well as to prove the efficiency of the proposed FLC compared with the traditional PI controller, particularly at low speeds.

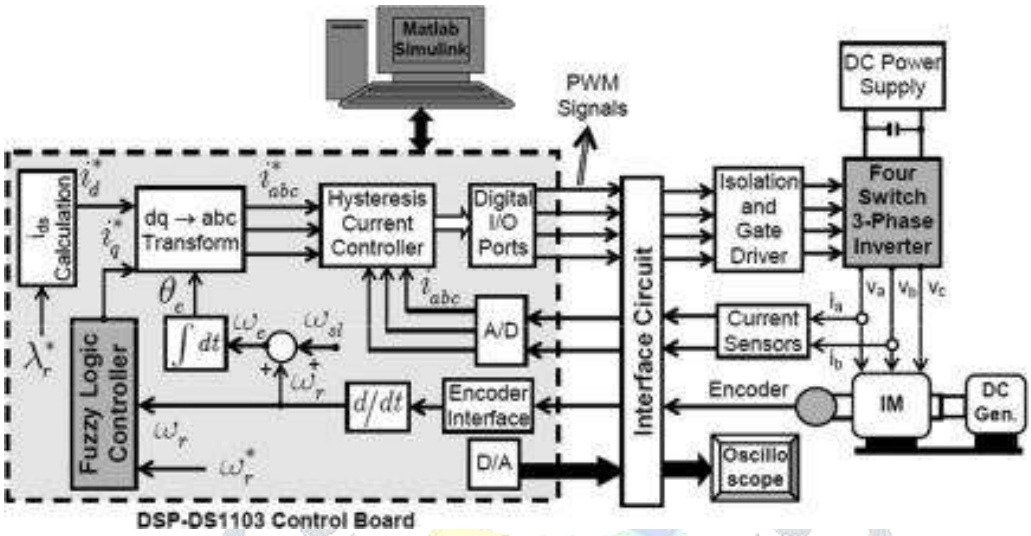

Fig. 14. Schematic diagram of the experimental system for FLC-based IFOC of an IM drive fed by FSTP inverter using DSP-DS1103 control board.

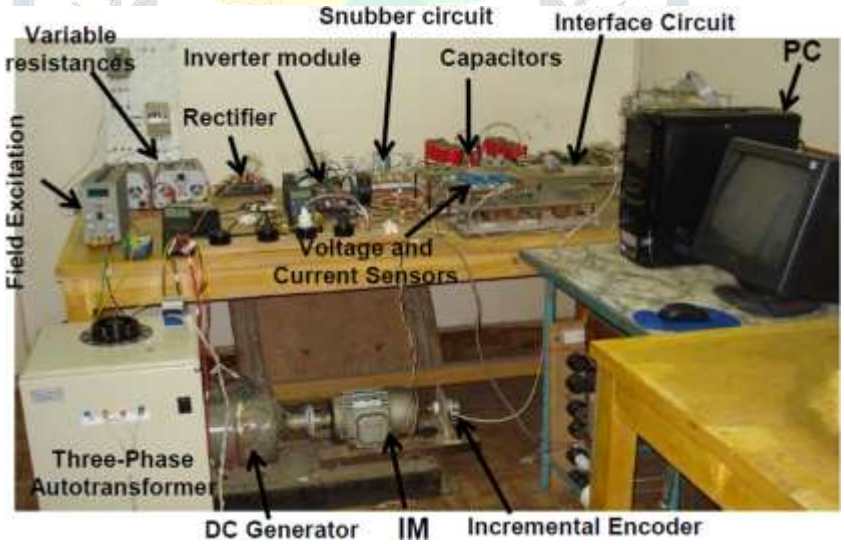

Fig. 15. Laboratory picture of an IM drive system using DSP-DS1103 control board.

Step Speed Reference Change: Fig. 16 demonstrates mo-tor speed and stator currents behavior of an FSTP inverter-fed IM drive for a starting operation at low speed with step speed ref-erence change from 0 to 100 r/min using the traditional PI con-troller (Fig. 16(a,b)) as well as the proposed FLC (Fig. 16 (c,d)). This figure is presented in comparison to the simulation results of Fig. 8. Another experimental result for the same variables is presented during the step speed reference change from 20 to 40 r/min as illustrated in Fig. 17. The experimental figures show that the FLC-based FSTP inverter-fed IM drive system has a good performance compared with the PI-based system. These results also illustrate that the transient response due to a sudden change in the reference speed can be handled fast without problems using the proposed FLC; whereas the PI controller has an over-shoot and the transient response is not fast compared to the FLC.

Speed Reversal: The two controllers are also tested exper-imentally under a speed reversal from 20 to −20 r/min as given in Fig. 18. This figure proves that the simplified FLC has a good speed tracking behavior during the speed reversal compared to the PI controller, which has overshoot and undershoot.

Sudden Load Impact: The robustness of the proposed FLC is examined under a sudden load change from light load to full load (7 N·m) when the reference speed equal to 20 r/min as illustrated in Fig. 19(b). The same result is taken with the PI controller as shown in Fig. 19(a). The superiority of the FLC is proved compared to the traditional PI controller. Since the FLC

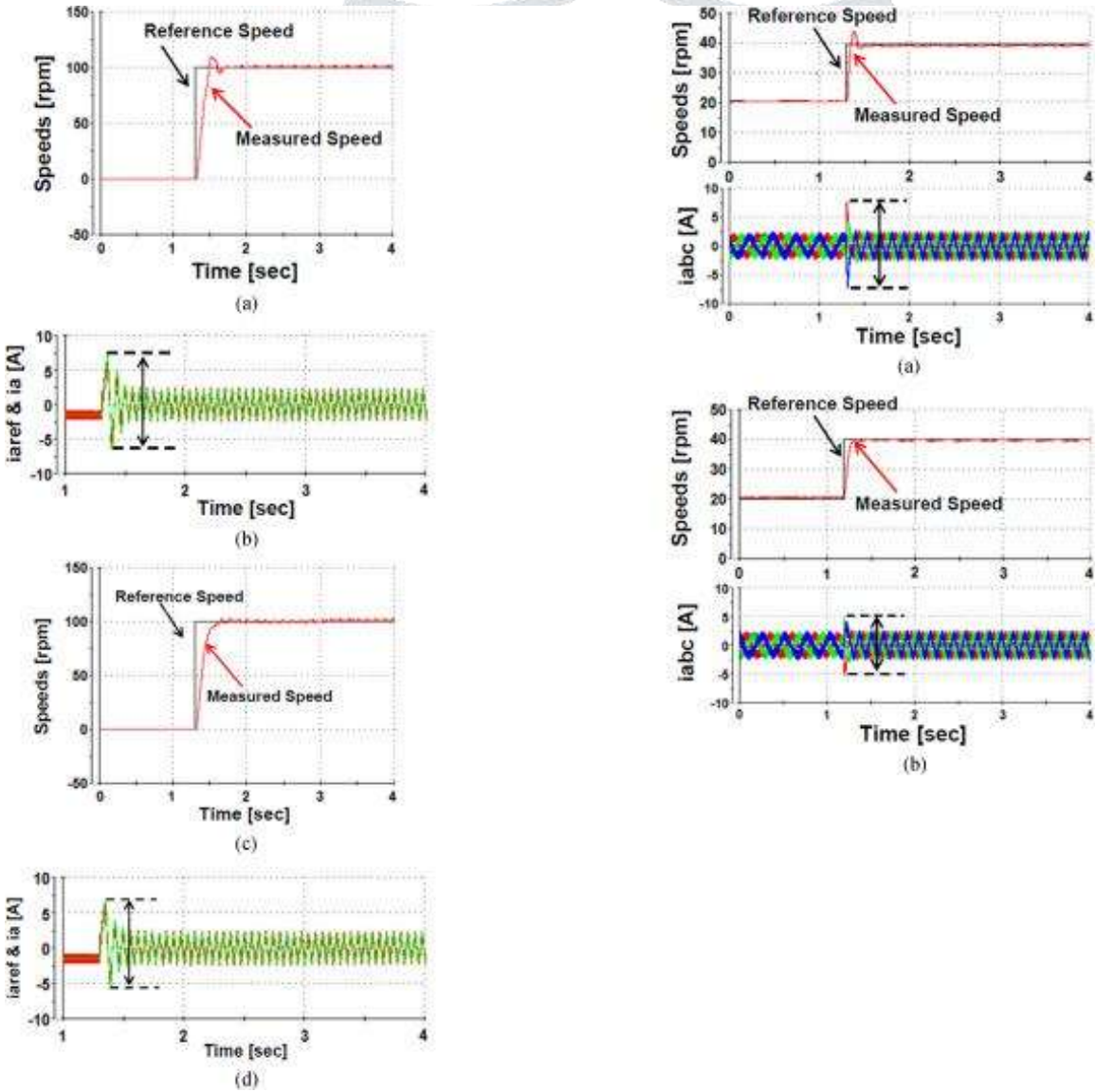

Fig. 17. Experimental speed and stator currents responses of an FSTP inverter-fed IM drive a step change of speed reference from 20 to 40 r/min using (a) traditional PI controller and (b) proposed FLC.

Fig.16.
Experimental speed and stator currents responses of an

achieves small speed dip and fast recovery time to its reference speed.

Parameters Variation: The performance of the two con-trollers under parameters variation is tested using inertia varia-tion as seen in Fig. 20(a) and (b) for both controllers. The results ensure that the FLC gives a good performance compared to the PI controller.

Table III shows a performance comparison between the FLC and PI controllers using the simulation and experimental results. This comparison includes the speed response, stator current, and torque disturbance. The performance of the two controllers is comparable in some cases. However, the FLC shows a good behavior than the PI controller.

The speed tracking capability of the FLC is investigated at low-speed operation. Thus, the proposed FLC-based drive

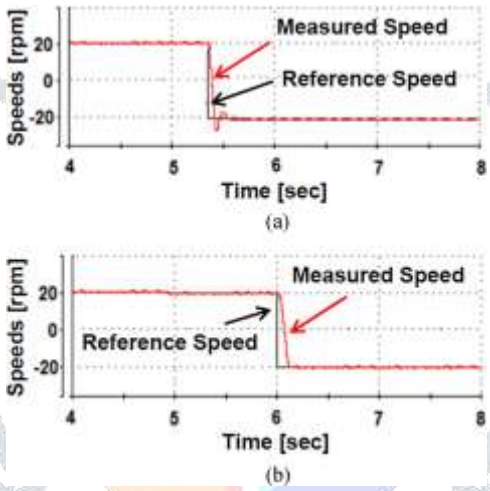

Fig. 18. Experimental speed responses of an FSTP inverter-fed IM drive under motor speed reverse at a speed reference from 20 r/min to -20 r/min using (a) traditional PI controller and (b) proposed FLC.

proves its superiority to the traditional PI-controller-based system under speed tracking, load disturbance, and parameters variation, and hence, the FLC is an accurate and robust controller for high-performance, low-power, and low-cost industrial applications.

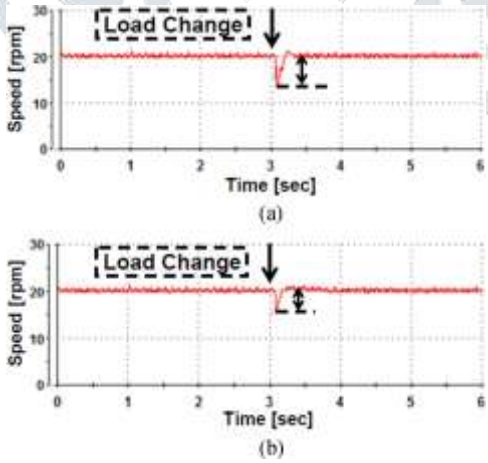

Fig. 19. Experimental speed responses of an FSTP inverter-fed IM drive under a sudden load change at a speed reference of 20 r/min using (a) traditional PI controller and (b) proposed FLC.

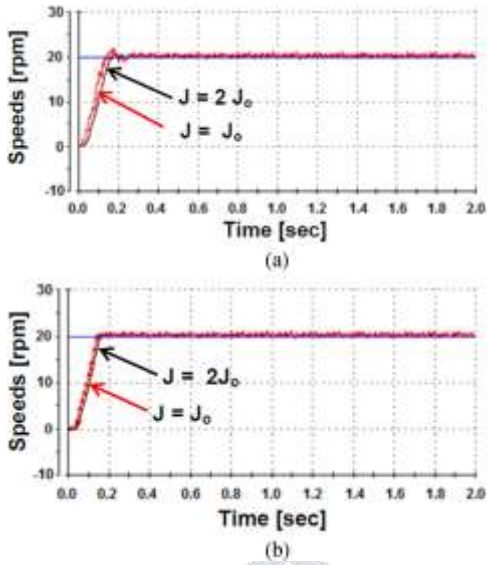

Fig. 20. Experimental speed responses of an FSTP inverter-fed IM drive motor under inertia mismatch at a speed reference of 20 r/min using (a) traditional PI controller and (b) proposed FLC

TABLE III
PERFORMANCE COMPARISON OF FLC AND PI CONTROLLER

IM Response		Simulation Results		Experimental Results	
		FLC	PI Controller	FLC	PI Controller
Speed Response	Rise Time	50 ms	50 ms	200 ms	200 ms
	Overshoot	0 r/min	20 r/min	1 r/min	12 r/min
	Settling Time	50 ms	300 ms	300 ms	320 ms
Stator Current	Starting	6 A	8 A	6.5 A	8 A
	Overshoot %	300%	400%	325%	400%
Torque	Speed dip	1 r/min	5 r/min	4 r/min	6 r/min
	Recovery time	150 ms	300 ms	250 ms	400 ms

VI. CONCLUSION

The proposed FLC-based IFOC for an IM drive fed by an FSTP inverter has been effectively implemented practically by the DSP-DS1103 control board for a laboratory 1.1-kW IM and by a computer simulation. The dynamic speed response of the IM drive at low speeds is improved using the FLC which is designed with low computation burden to be appropriate for real-time applications. The validity of the proposed FLC has been examined both in simulation and experimentation at vari-ous speed reference tracking and load torque disturbances, par-ticularly at low speeds. To confirm the efficacy of the proposed controller, a fair performance comparison of the proposed FLC-based IM drive with a PI controller has been presented. The robustness of the two controllers has been also examined under parameters variation, especially motor inertia, and stator and rotor resistances. Comparative simulation and experimental re-sults demonstrate that the proposed FLC of an FSTP inverter-fed IM drive is superior to the PI controller under speed tracking, load disturbances, and parameters variation. The usefulness of the FLC has been verified by its high dynamic speed response without overshoot and undershoot, and with zero steady-state error, and less THD of stator currents. This shows the good ca-pability of the FLC-based IM drive fed by an FSTP inverter for cost-effective low-power industrial applications.

APPENDIX

TABLE IV

PARAMETERS OF IM

		Stator leakage	0.0221
Rated power	1.1 kW	inductance	H
			0.4114
Rated current	2.545 A	Mutual inductance	H
No. of poles	4	Supply frequency	50 Hz
	7.4826		
Stator resistance	Ω	Supply voltage	380 V
	3.6840		0.02
Rotor resistance	Ω	Inertia	$kg{\cdot}m^2$
Rotor leakage	0.0221		
inductance	H	Rated voltage	380 V

REFERENCES

[1] H. W. van der Broeck and J. D. van Wyk, "A comparative investigation of three-phase induction machine drive with a component minimized voltage-fed inverter under different control options," *IEEE Trans. Ind. Appl.*, vol. IA-20, no. 2, pp. 309–320, Mar./Apr. 1984.

[2] P. Enjeti and A. Rahman, "A new single-phase to three-phase converter with active input current shaping for low cost ac motor drives," *IEEE Trans. Ind. Appl.*, vol. 29, no. 4, pp. 806–813, Jul./Aug. 1993.

[3] C. B. Jacobina, M. B. R. Correa, E. R. C. da Silva, and A. M. N. Lima, "Induction motor drive system for low power applications," *IEEE Trans. Ind. Appl.*, vol. 35, no. 1, pp. 52–61, Jan./Feb. 1999.

[4] C.-T. Lin, C.-W. Hung, and C.-W. Liu, "Position sensorless control for four-switch three-phase brushless DC motor drives," *IEEE Trans. Power Electron.*, vol. 23, no. 1, pp. 438–444, Jan. 2008.

[5] S. B. Ozturk, W. C. Alexander, and H. A. Toliyat, "Direct torque control of four-switch brushless DC motor with non-sinusoidal back EMF," *IEEE Trans. Power Electron.*, vol. 25, no. 2, pp. 263–271, Feb. 2010.

[6] C. Xia, Z. Li, and T. Shi, "A control strategy for four-switch three-phase brushless DC motor using single current sensor," *IEEE Trans. Ind. Elec-tron.*, vol. 56, no. 6, pp. 2058–2066, Jun. 2009.

[7] M. Masmoudi, B. El Badsi, and A. Masmoudi, "DTC of B4-Inverter-Fed BLDC motor drives with reduced torque ripple during sector-to sector commutations," *IEEE Trans. Power Electron.*, vol. 29, no. 9, pp. 4855–4865, Sep. 2014.

[8] K. D. Hoang, Z. Q. Zhu, and M. P. Foster, "Influence and compensation of inverter voltage drop in direct torque-controlled four-switch three-phase PM brushless AC drives," *IEEE Trans. Power Electron.*, vol. 26, no. 8, pp. 2343–2357, Aug. 2011.

[9] B. El Badsi, B. Bouzidi, and A. Masmoudi, "DTC scheme for a four-switch inverter-fed induction motor emulating the six-switch inverter operation," *IEEE Trans. Power Electron.*, vol. 28, no. 7, pp. 3528–3538, Jul. 2013.

[10] S. Dasgupta, S. N. Mohan, S. K. Sahoo, and S. K. Panda, "Ap-plication of four-switch-based three-phase grid-connected inverter to connect renewable energy source to a generalized unbalanced micro-grid system," *IEEE Trans. Ind. Electron.*, vol. 60, no. 3, pp. 1204–1215, Mar. 2013.

[11] W. Wang, A. Luo, X. Xu, L. Fang, T. Minh Chau, and Z. Li, "Space vector pulse-width modulation algorithm and DC-side voltage control strategy of three-phase four-switch active power filters," *IET Power Electron.*, vol. 6, no. 1, pp. 125–135, Jan. 2013.

[12] X. Tan, Q. Li, H. Wang, L. Cao, and S. Han, "Variable parameter pulse width modulation-based current tracking technology applied to four switch three-phase shunt active power filter," *IET Power Electron.*, vol. 6, no. 3, pp. 543–553, Mar. 2013.

[13] F. Blaabjerg, D. O. Neacsu, and J. K. Pedersen, "Adaptive SVM to compensate dc-link voltage ripple for four-switch, three-phase voltage source inverter," *IEEE Trans. Power Electron.*, vol. 14, no. 4, pp. 743–751, Jul. 1999.

[14] R. Wang, J. Zhao, and Y. Liu, "A comprehensive investigation of four switch three-phase voltage source inverter based on double Fourier integral analysis," *IEEE Trans. Power Electron.*, vol. 26, no. 10, pp. 2774–2787, Oct. 2011.

[15] M. B. R. Correa, C. B. Jacobina, E. R. C. Da Silva, and A. M. N. Lima, "A general PWM strategy for four-switch three phase inverters," *IEEE Trans. Power Electron.*, vol. 21, no. 6, pp. 1618–1627, Nov. 2006.

B.Bhaskar. Asst.Professor, Department of EEE in Chaitanya Institute of Technology & Science, Kakatiya University, Hanamkonda, Warangal, Telangana, India.

L.Raju. Pursuing M.Tech (PE), Department of EEE in Chaitanya Institute of Technology & Science, Kakatiya University, Hanamkonda, Warangal, Telangana, India.